SUPPLEMENTARY DATA

Adsorption and Corrosion Inhibition Mechanism of Schiff Base Conjugated Oligoelectrolyte on Mild Steel in Acidic Media: Electrochemical and Surface Characterization Studies

Lalita Thakur[a], Irshad Mohiuddin[b], Raghubir Singh[c*], Varinder Kaur[a*]

[a] *Department of Chemistry & Centre for Advanced Studies in Chemistry, Panjab University, Chandigarh–160014, India*

[b] *Department of Chemistry and Biochemistry, Thapar Institute of Engineering and Technology, Patiala, Punjab-147004, India*

[c] *Department of Chemistry, DAV College, Sector 10, Chandigarh-160011, India*

Corresponding author: var_ka04@yahoo.co.in (V.K.), raghubirsingh@davchd.ac.in (R.S.)

Table of Contents

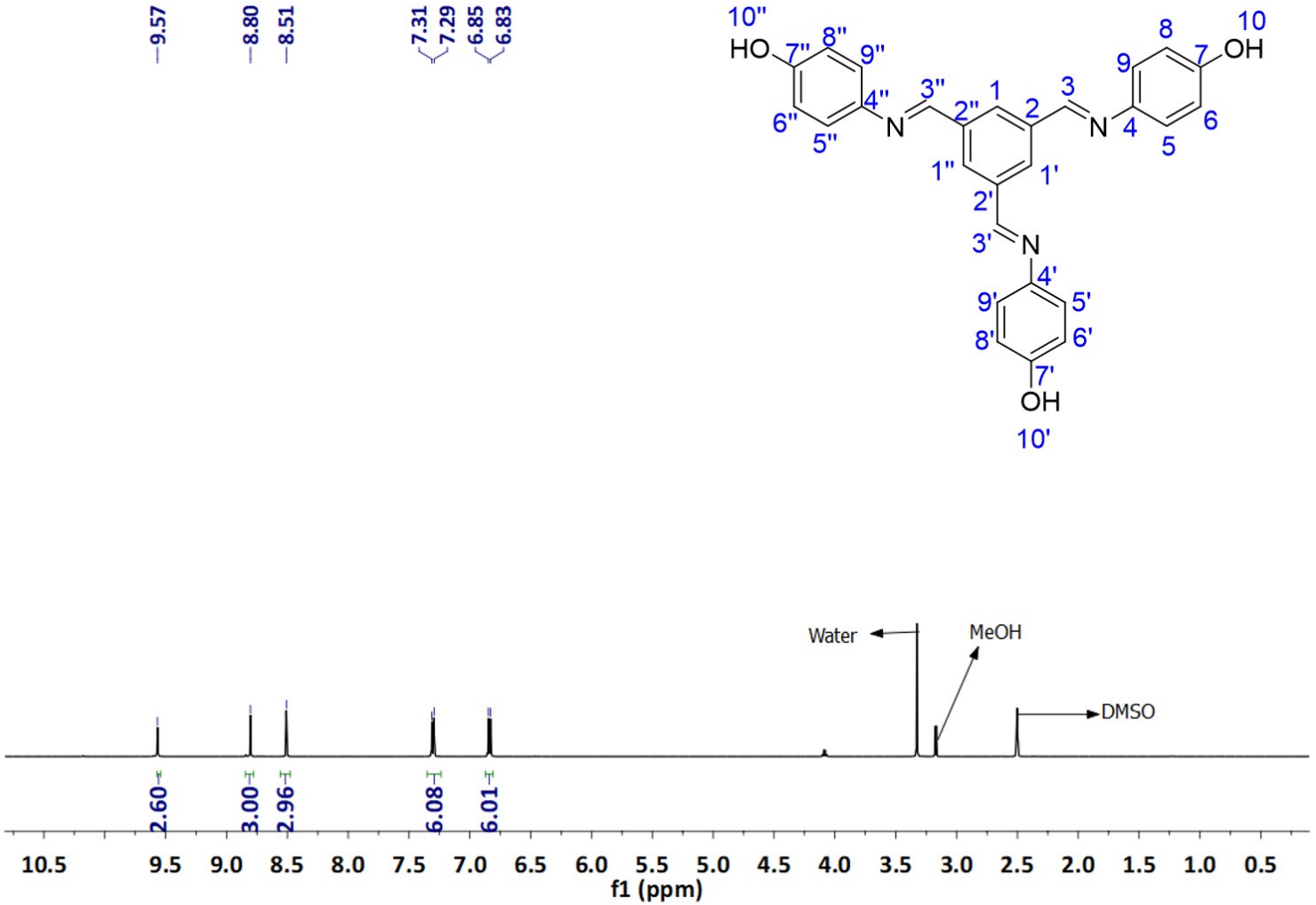

Figure S1 ^{1}H NMR spectrum of BTC-SB

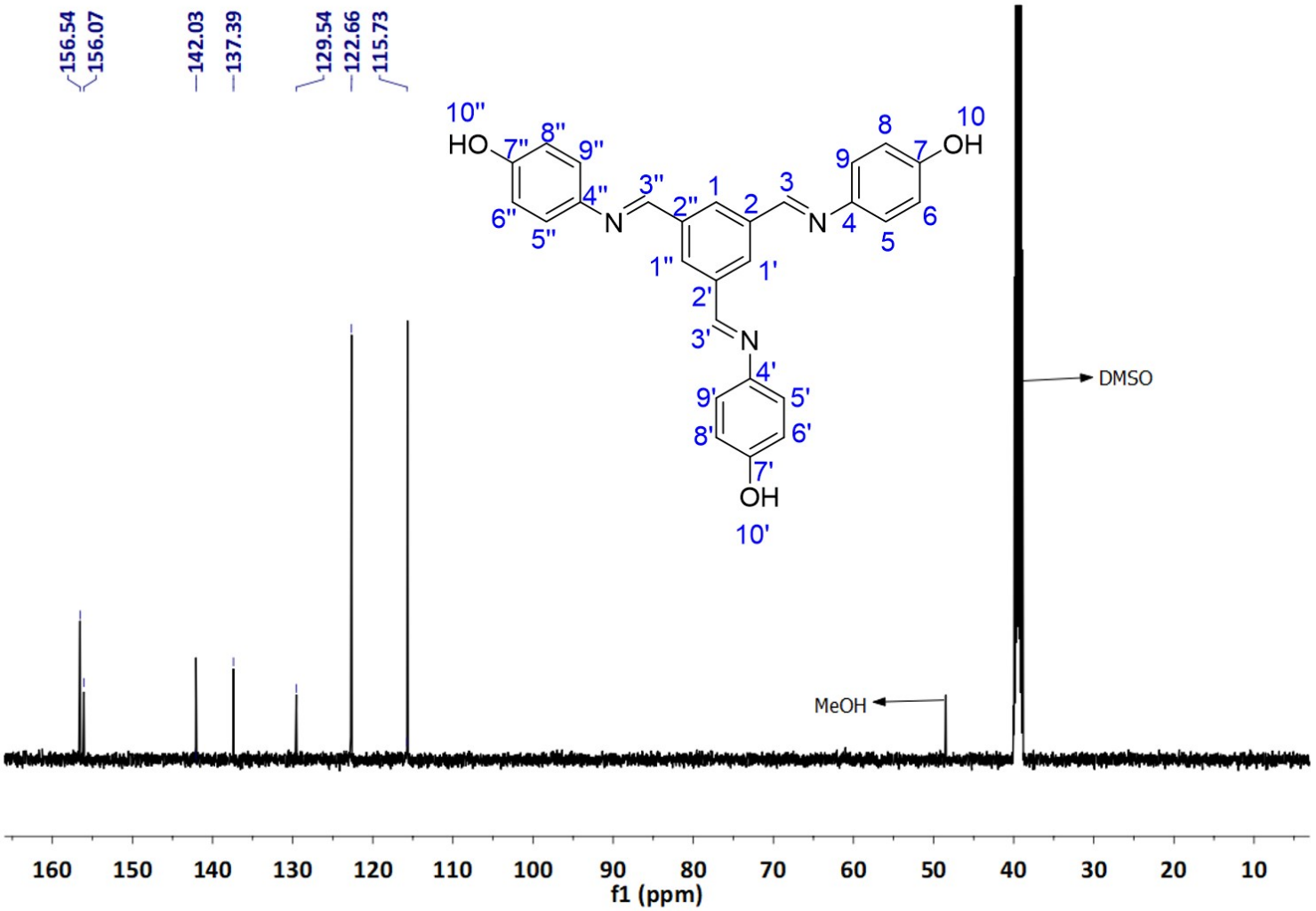

Figure S2 ^{13}C NMR spectrum of BTC-SB

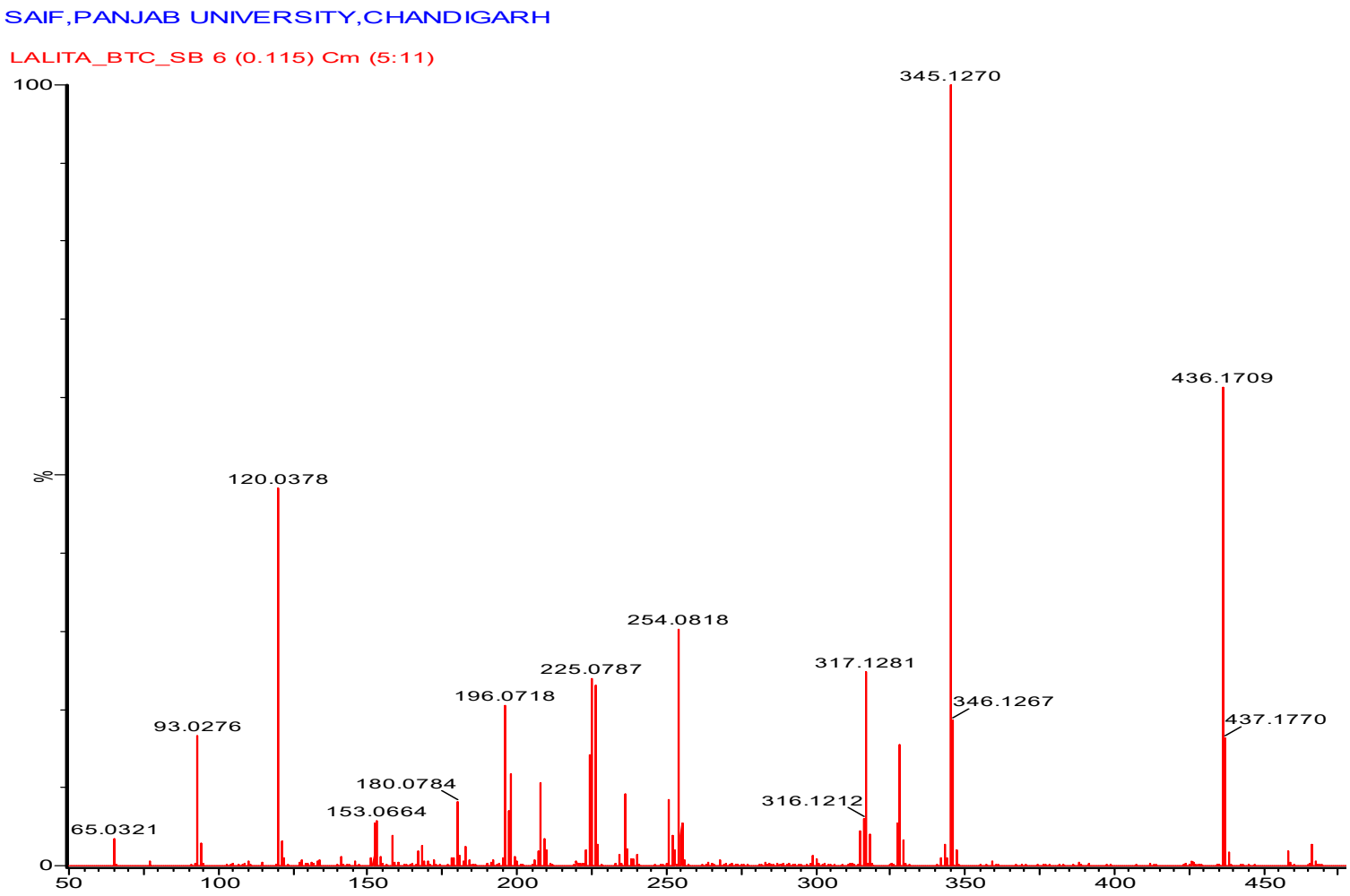

Figure S3 Mass spectrum of BTC-SB

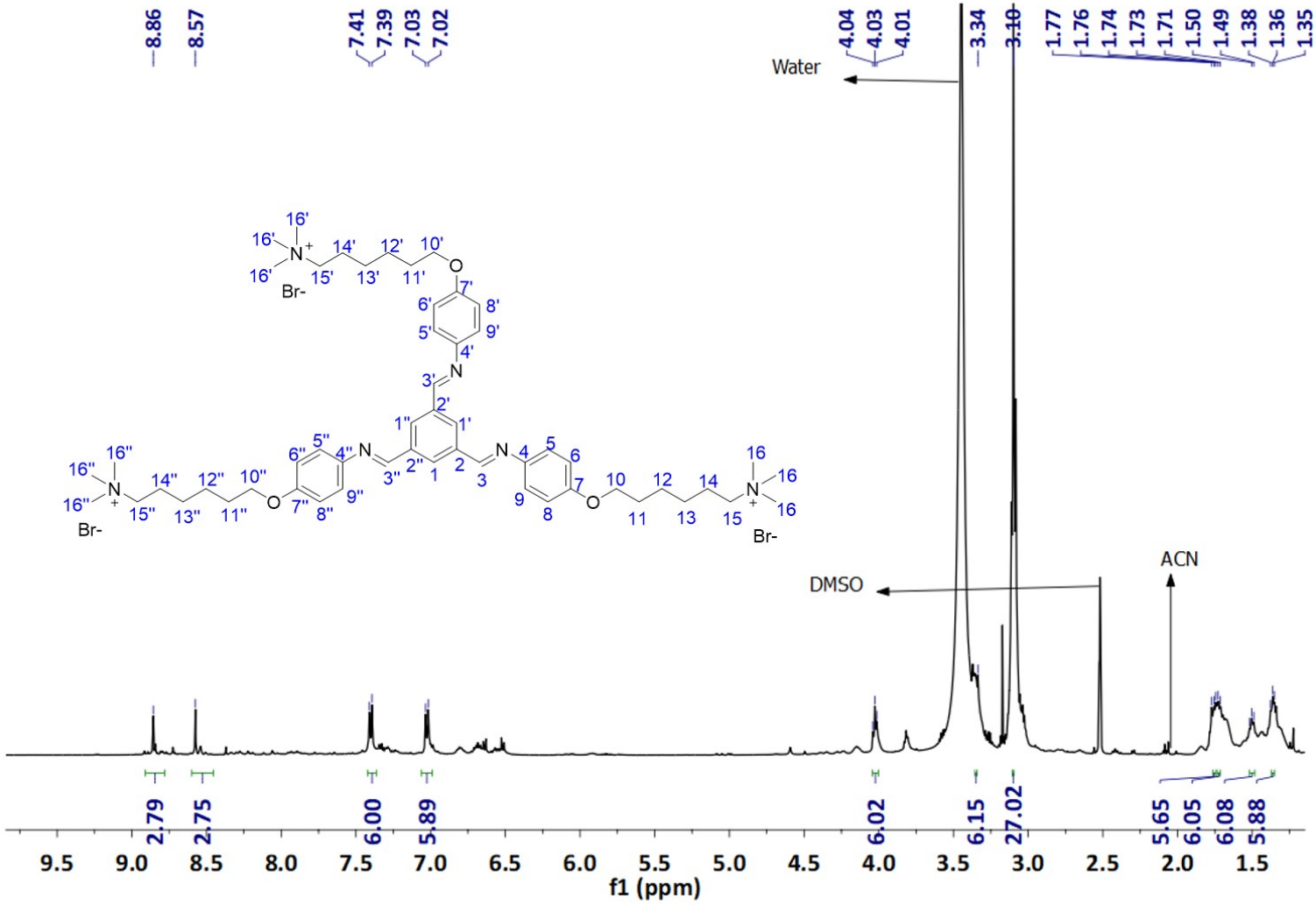

Figure S4 ^{1}H NMR spectrum of BTC-SBCOE

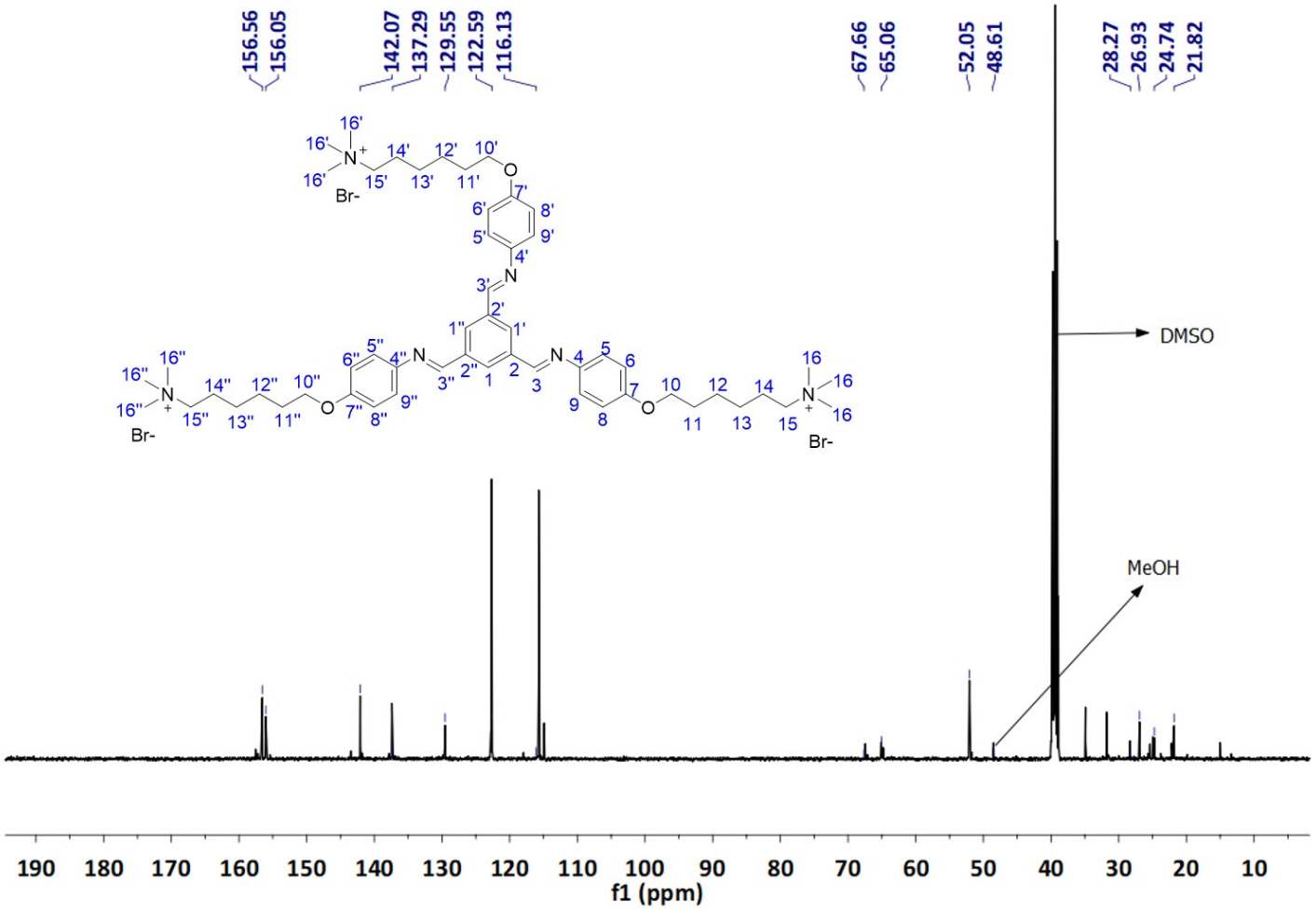

Figure S5 ^{13}C NMR spectrum of BTC-SBCOE

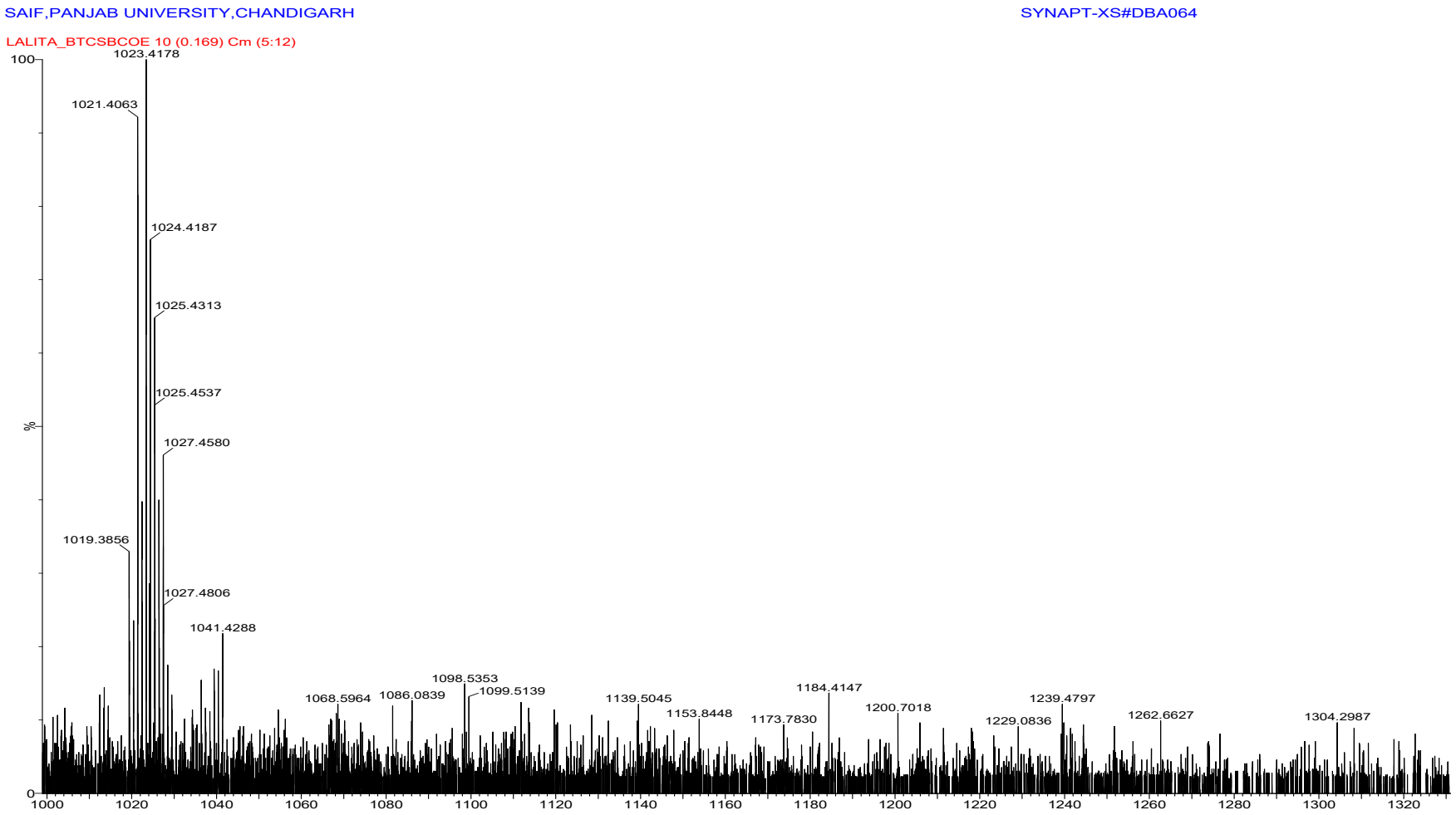

Figure S6 (a) Mass spectrum of BTC-SBCOE

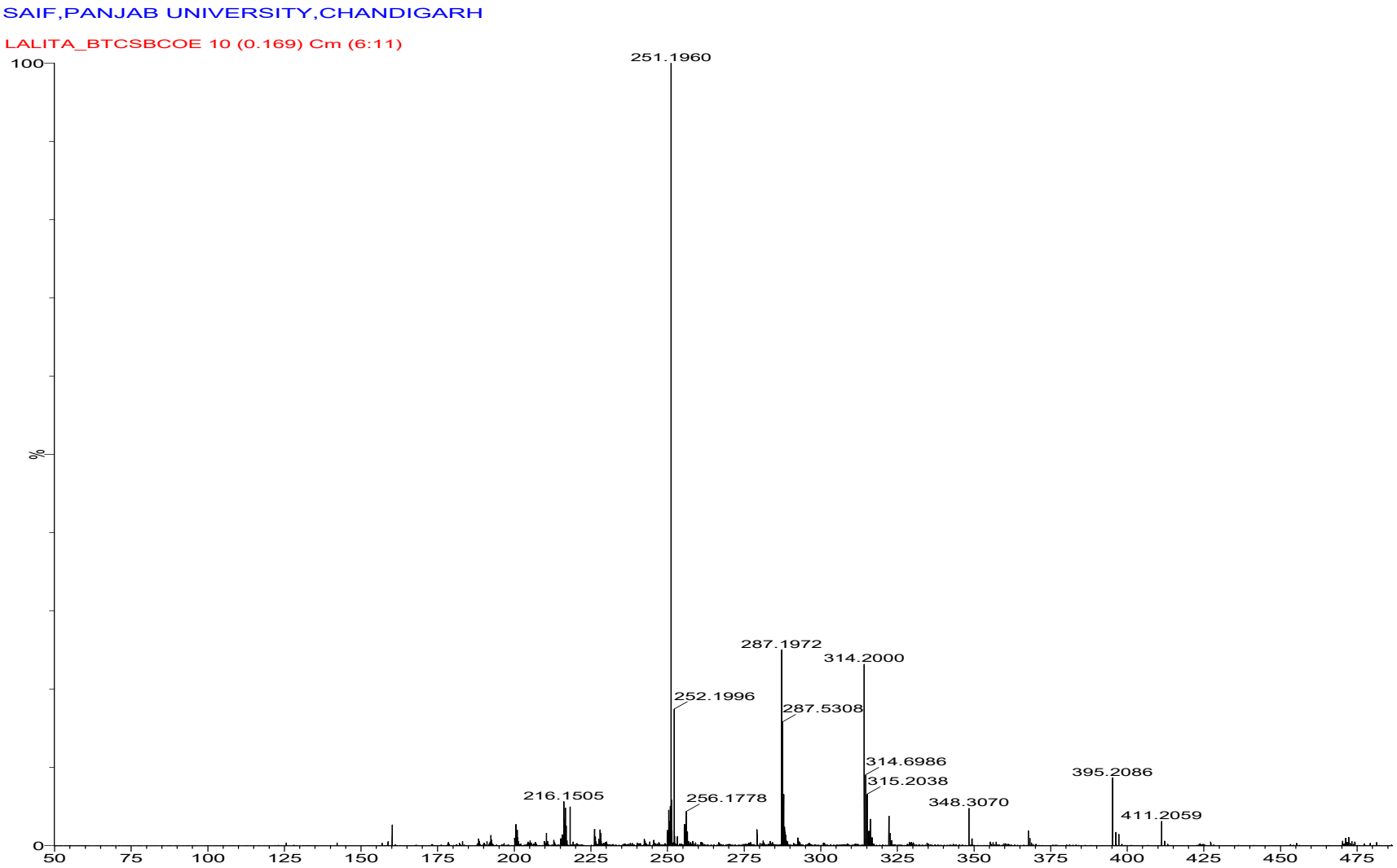

Figure S6 (b) Mass spectrum of BTC-SBCOE

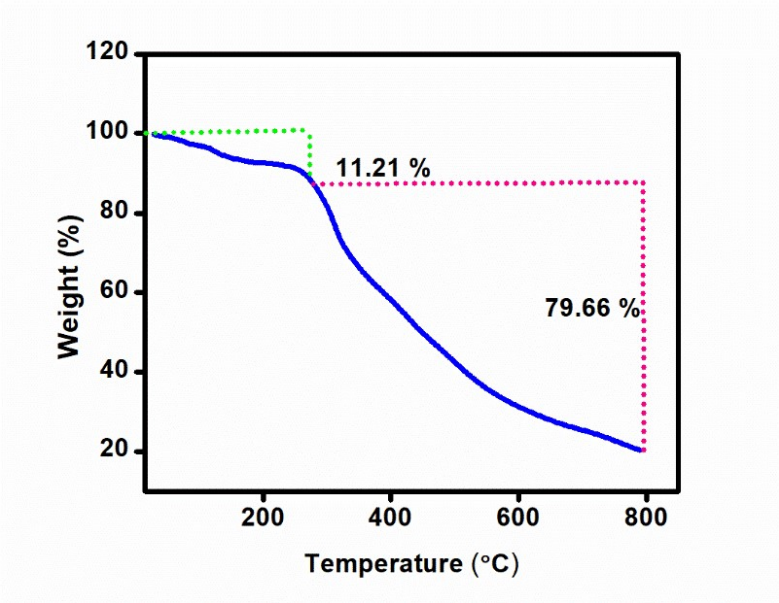

Figure S7 TGA plot of BTC-SBCOE

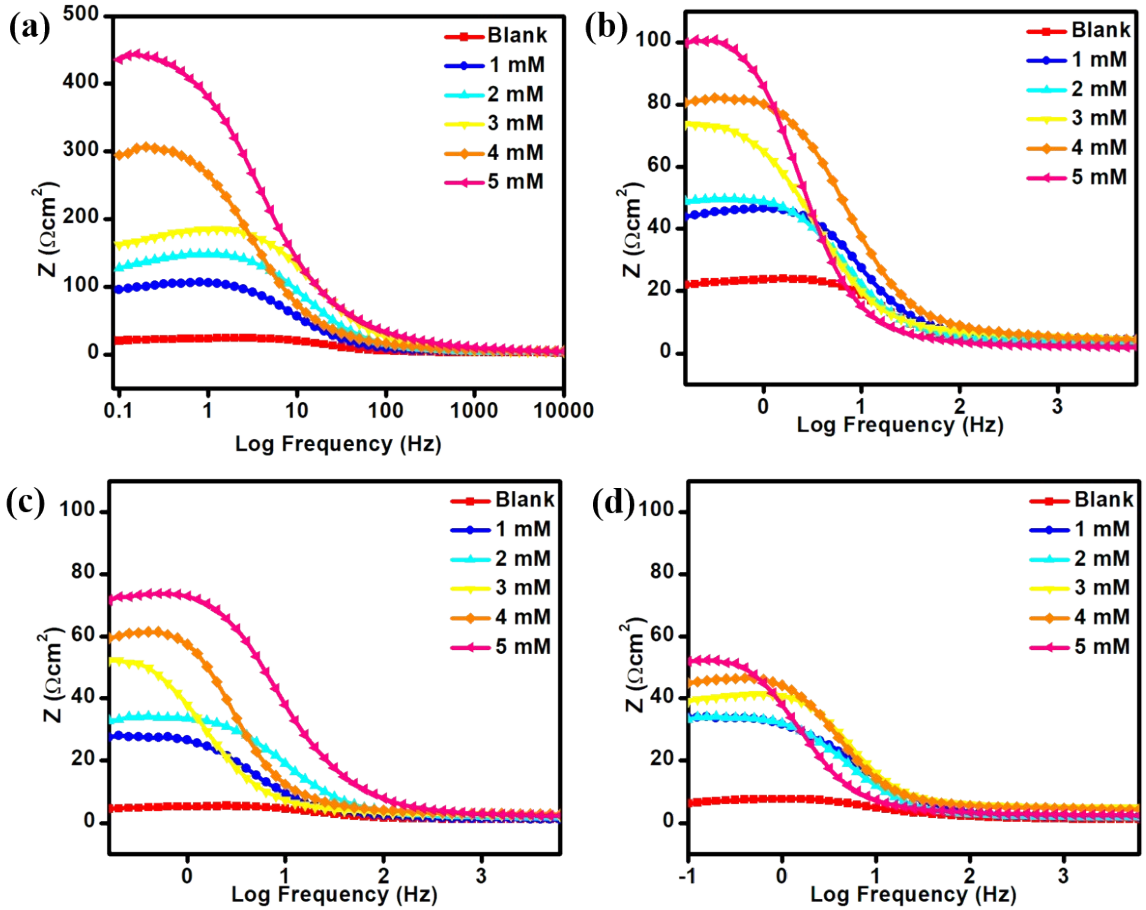

Figure S8 Bode curves for mild steel in the 2M HCl solution for the blank and with different concentrations of the BTC-SBCOE solution at **(a)** 25 ˚C, **(b)** 40 ˚C, **(c)** 60 ˚C, and **(d)** 80 ˚C

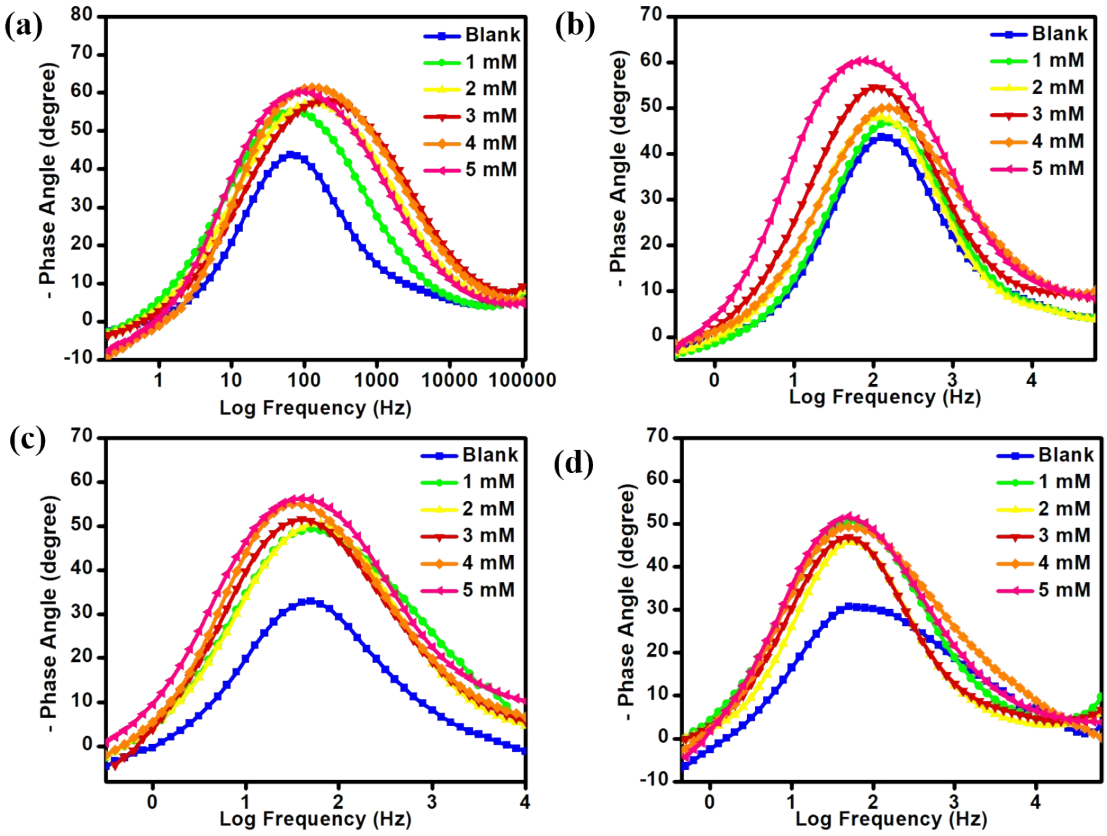

Figure S9 Phase angle plot for mild steel in the 2M HCl solution for the blank and with different concentrations of the BTC-SBCOE solution at **(a)** 25 ˚C, **(b)** 40 ˚C, **(c)** 60 ˚C, and **(d)** 80 ˚C

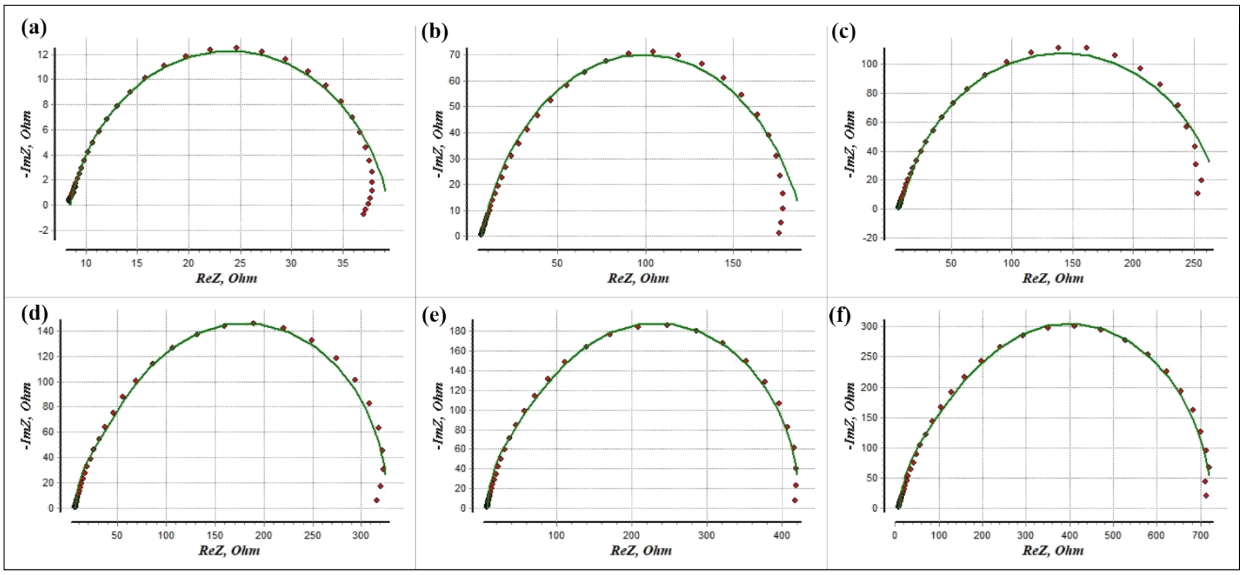

Figure S10 EIS fitting of data for **(a)** blank **(b)** 1, **(c)** 2, **(d)** 3, **(e)** 4, and **(f)** 5mM of BTC-SBCOE at 25˚C

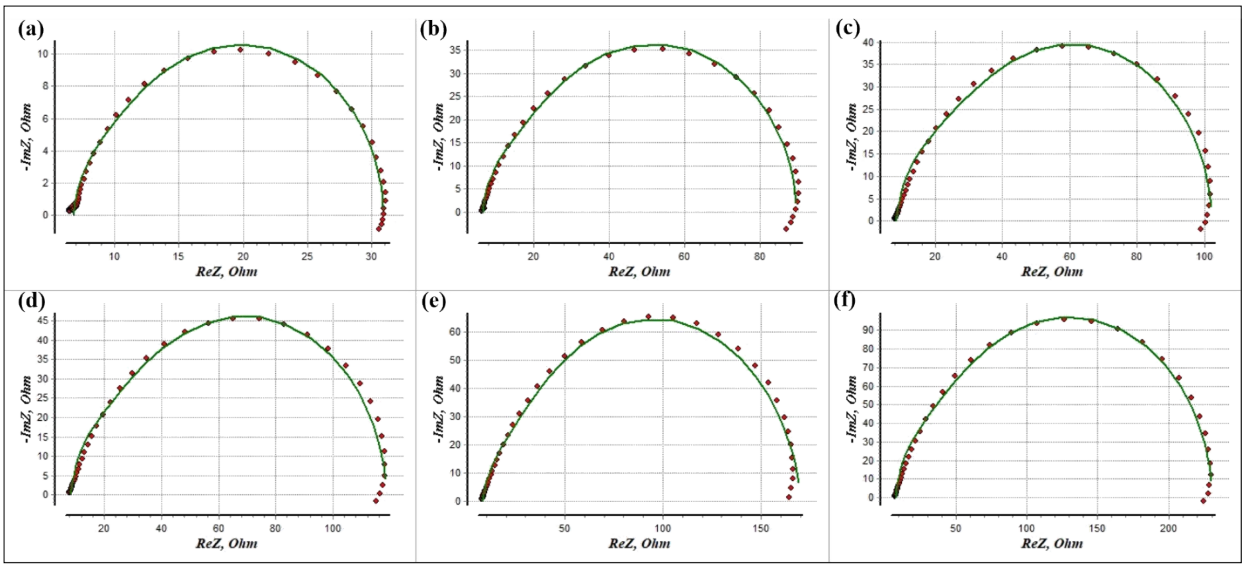

Figure S11 EIS fitting of data for **(a)** blank **(b)** 1, **(c)** 2, **(d)** 3, **(e)** 4, and **(f)** 5mM of BTC-SBCOE at 40˚C

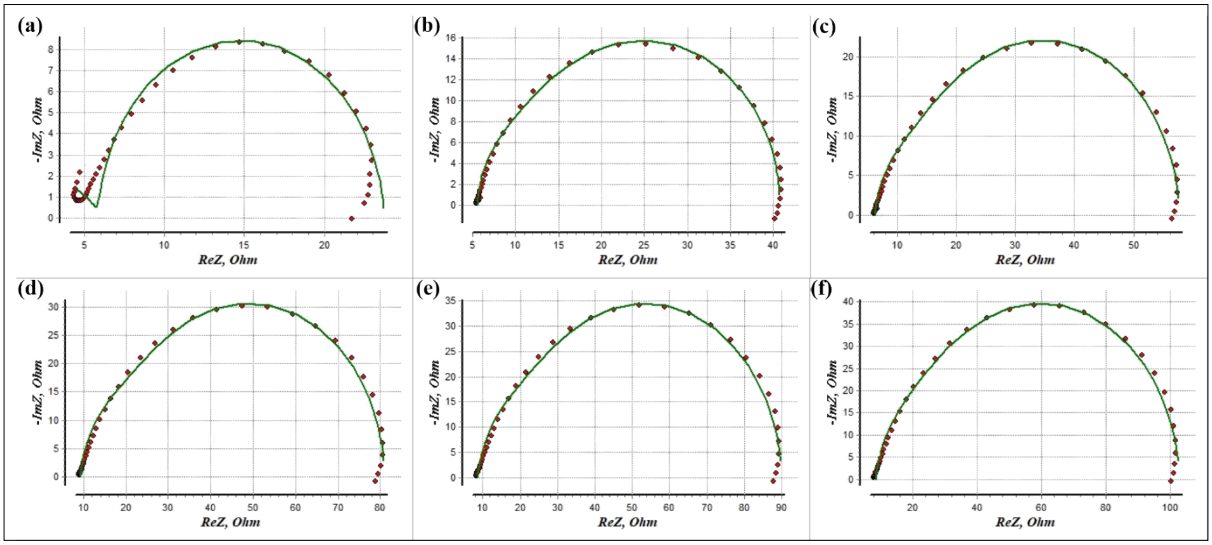

Figure S12 EIS fitting of data for **(a)** blank **(b)** 1, **(c)** 2, **(d)** 3, **(e)** 4, and **(f)** 5mM of BTC-SBCOE at 60˚C

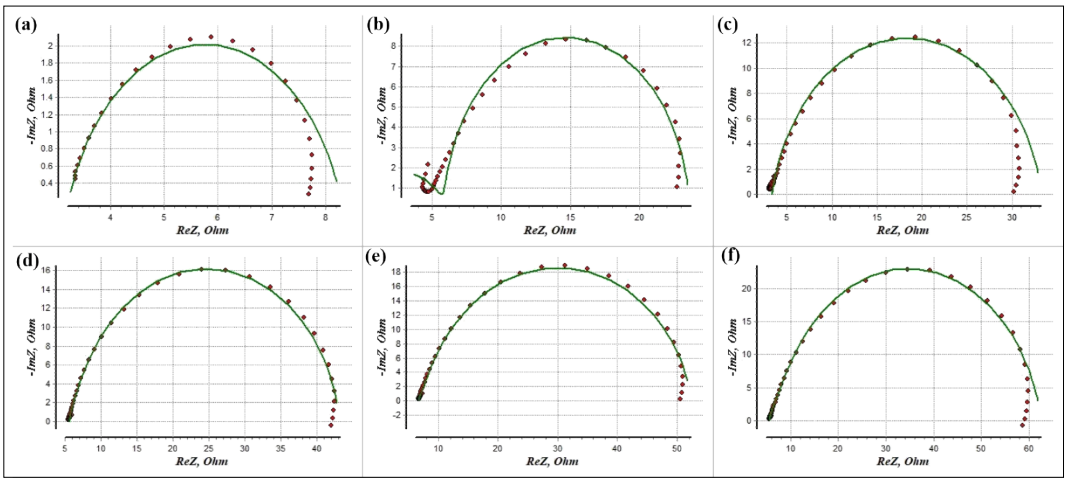

Figure S13 EIS fitting of data for **(a)** blank **(b)** 1, **(c)** 2, **(d)** 3, **(e)** 4, and **(f)** 5mM of BTC-SBCOE at 80˚C

Table S1. PDP parameters, i.e., corrosion current density **(i_{corr})**, anodic Tafel **(β_a)** and cathodic Tafel slopes **(β_c),** polarization resistance **(R_p),** mild steel in the 2M HCl medium in the presence of 1 to 5 mM concentration of BTCSB-COE in comparison to blank at different studied temperatures (40 ˚C, 60 ˚C, and 80 ˚C)

Sr. No.	T (°C)	C (mM)	$-E_{corr}$ (mV vs. Ag/AgCl)	i_{corr} (mA cm^{-2})	β_a (mV/ decade)	$-\beta_c$ (mV/ decade)	R_p (Ω cm^2)	IE%
1	40	-	448	1.31	15.12	10.1	2.00	-
2		1	428	0.20	9.41	8.12	9.46	84.35
3		2	416	0.17	8.6	7.8	10.44	87.02
4		3	409	0.16	8.1	7.42	10.50	87.40
5		4	403	0.14	6.96	7.5	11.19	88.93
6		5	383	0.12	5.41	7.8	11.55	90.45
7	60	-	431	1.96	8.28	9.26	0.96	-
8		1	419	0.29	7.58	7.97	5.81	85.20
9		2	413	0.26	6.18	7.8	5.75	86.73
10		3	409	0.24	6.37	7.6	6.29	87.75
11		4	404	0.20	5.8	8.9	7.62	89.79
12		**5**	**401**	**0.07**	**5.2**	**6.82**	**18.30**	**96.42**
13	80	-	419	2.77	7.4	7.92	0.59	-
14		1	416	0.45	7.1	7.02	3.40	83.75
15		2	411	0.40	6.8	6.93	3.72	85.55
16		3	395	0.31	5.5	6.54	4.18	88.80

17	4	393	0.29	8.49	5.9	5.21	89.53
18	5	389	0.19	9.4	11.44	11.79	93.14

Table S2. Electrochemical impedance parameters like solution resistance **(R_s),** double layer capacitance (***C_{dl}*),** charge transfer resistance **(*R_{ct}*)**, inhibition efficiency for mild steel in 2 M HCl solution in absence and presence of 1 to 5 mM of BTC-SBCOE at 40 ˚C, 60 ˚C, and 80 ˚C

Sr. No.	**T (°C)**	**C (mM)**	**R_s (Ωcm^2)**	**R_{ct} (Ωcm^2)**	***CPE_{dl}***		**CPE_f**		**R_f**	**$R_p = R_{ct} + R_s$ (Ω cm^2)**	**Cdl(µF cm^{-2})**	**IE%**
					***Y_O*×10^{-6} (Ω^{-1} cm^{-2})**	***n***	**Y_O×10^{-6} (Ω^{-1} cm^{-2})**	**n**				
1	40	-	3.04	7.670	600	0.90	-	-	-	10.67	286.58	-
2		1	3.60	37.55	587	0.87	276	0.88	1.50	41.15	230.66	74.07
3		2	3.98	45.57	500	0.88	189	0.88	1.95	49.55	211.67	78.46
4		3	4.96	71.38	495	0.87	154	0.87	2.13	76.34	199.64	86.02
5		4	4.38	78.347	164	0.84	132	0.89	5.10	82.72	40.880	87.10
6		5	4.71	102.2	152	0.82	126	0.87	1.13	106.91	30.700	90.01
7	60	-	1.20	3.570	610	0.98	-	-	-	4.77	523.32	-
8		1	1.30	22.36	530	0.97	289	0.91	3.40	23.66	449.36	79.83
9		2	2.01	30.78	520	0.92	192	0.89	7.10	32.78	306.17	85.44
10		3	2.44	36.14	500	0.90	176	0.89	1.90	38.58	235.64	87.63
11		4	2.94	55.50	415	0.91	158	0.89	1.30	58.44	212.65	91.83
12		5	1.80	71.80	423	0.89	149	0.89	1.10	73.60	173.61	93.51
13	80	-	1.30	4.000	810	0.97	-	-	-	5.3	650.14	-
14		1	1.39	23.66	650	0.95	283	0.87	3.74	25.05	448.11	78.84
15		2	1.90	24.21	589	0.91	213	0.88	7.91	26.11	298.53	79.70
16		3	5.00	37.02	570	0.89	187	0.88	9.20	42.02	271.95	87.38
17		4	4.40	42.15	486	0.88	179	0.88	5.10	46.55	207.33	88.61
18		5	3.80	47.65	432	0.89	167	0.88	2.60	51.45	193.72	89.69

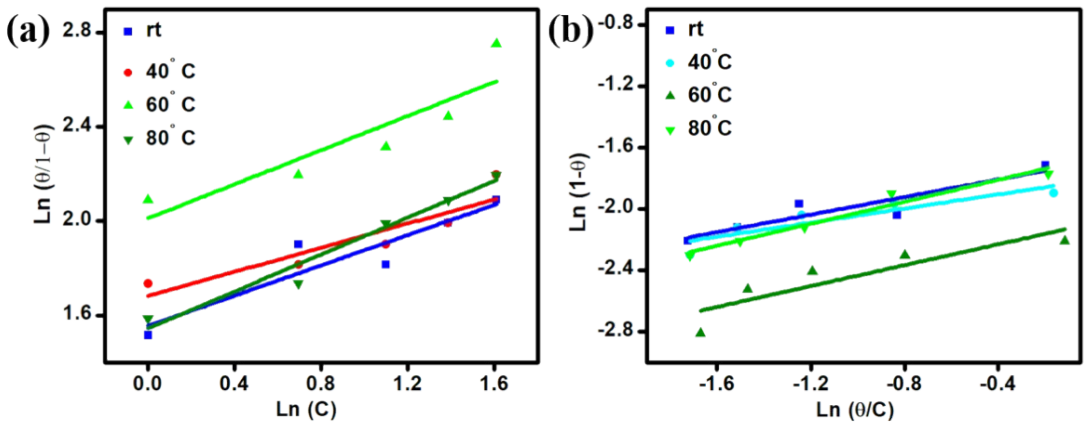

Figure S14 (a) El-Awady, and **(b)** Flory-Huggins isotherms to examine the interaction of BTC-SBCOE with the MS surface

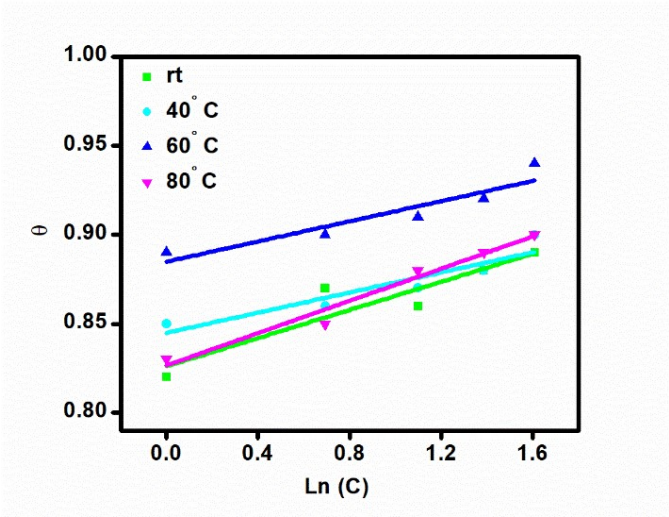

Figure S15 Temkin isotherm to examine the interaction of BTC-SBCOE with the MS surface

Table S3. The thermodynamic parameter of BTC-SBCOE as calculated from the El-Awady, Flory-Huggins, and Temkin adsorption isotherms

	El-Awady adsorption model				**Flory-Huggins adsorption model**				**Temkin adsorption model**			
T (° C)	**K_{ads} (×10^3)**	**ΔG_{ads} (kJ/mol)**	**R^2**	**Slope**	**K_{ads} (×10^3)**	**ΔG_{ads} (kJ/mol)**	**R^2**	**Slope**	**K_{ads} (×10^3)**	**ΔG_{ads} (kJ/mol)**	**R^2**	**Slope**
rt	35.9	-42.37	0.8	0.32	0.02	-24.15	0.80	0.28	6.70	-38.28	0.81	0.03

	3		2									
40	48.14	-46.03	0.77	0.25	0.01	-25.08	0.75	0.23	6.99	-41.01	0.82	0.02
60	102.90	-51.07	0.74	0.36	0.00	-24.89	0.72	0.33	7.67	-43.89	0.82	0.02
80	35.05	-50.98	0.95	0.39	0.02	-29.27	0.94	0.35	6.70	-46.13	0.96	0.04

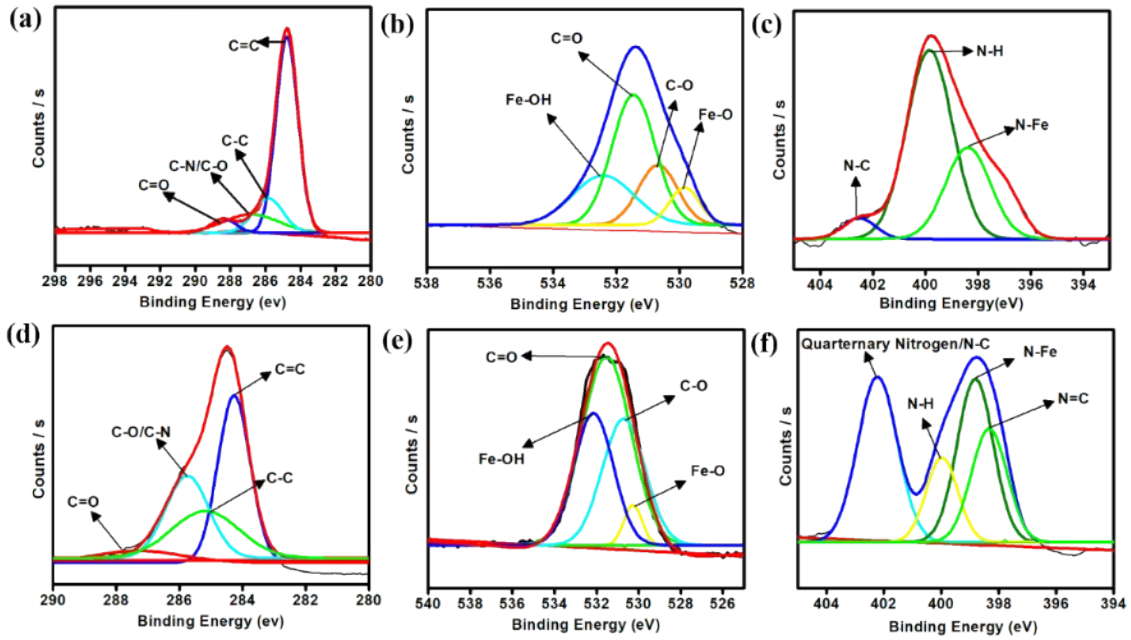

Figure S16 XPS survey of mild steel **(a)** The high-resolution C 1s **(b)** O 1s, and **(c)** N 1s spectrum of mild steel without corrosion inhibitor BTC-SBCOE. **(d)** The high-resolution C1s, **(e)** O 1s, and **(f)** N 1s spectrum of mild steel with corrosion inhibitor BTC-SBCOE

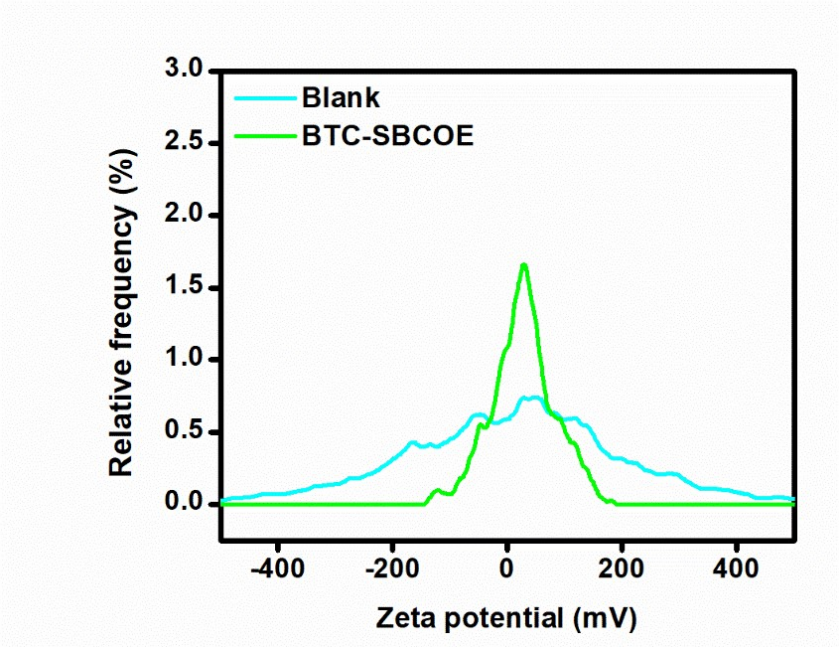

Fig. S17 Zeta potential of blank solution and after immersion of BTC-SBCOE in acidic medium

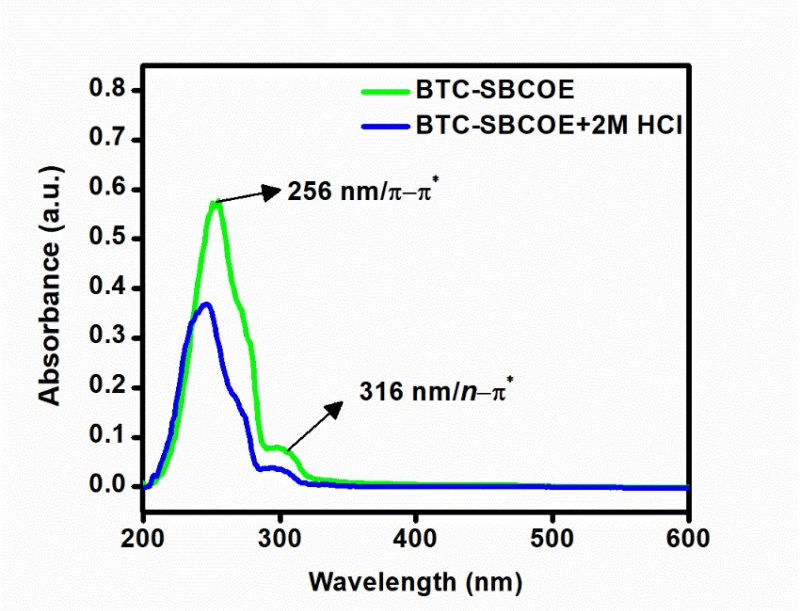

Fig. S18 UV-vis spectra of BTC-SBCOE before and after immersion in acidic medium

Table S4. Inhibition activity comparison of different corrosion inhibitors as compared to BTC-SBCOE in different acidic media

S. No.	Inhibitor	Conc.	Type of solution	Efficiency at room temperature	Efficiency at higher temperature	Type of adsorption	Ref
1	Sodium Cocoyl Glycinate	0.2864 mM	1M HCl	95.21 %	73.21 %	Mixed type	33
2	Long chain fatty hydrazides	50 mg/L	1M HCl	90.94 %	-	Cathodic type	34
3	Sunflower head pectin	2.0 M	1M HCl	92.05 %	90.30 %	Mixed type	35
4	Furfuryl alcohol	136×10^{-5} M	15 % HCl	95.40%	90.08 %	Mixed type	36
5	Choline amino acid	600 ppm	1M HCl	95.2 %	-	Mixed type	37
6	2-(4-(4,5-dihydro-3-(4-methoxyphenyl)-1H-pyrazol-5-yl) phe noxy) acetic acid (PYR-1)	5 mM	1M HCl	94.01 %	Above 90 %	Mixed type	38
7	2-(4-(4,5-dihydro-3-(4-methoxyphenyl)-1H-pyrazol-5-yl)phe noxy)acetic acid (PYR-1) and 2-(4-(4,5-dihydro-3-p-tolyl-1H-pyrazol-5-yl)phenoxy)acetic acid (PYR-2)	5 mM	1M HCl	88.00 %	Above 90 %	Mixed type	38
8	Azo-Cum	0.5 mM	1M HCl	80.25 %		Mixed type	39
9	Laurhydrazide N-propane-3-one	20 mM	5M HCl	94.00 %	61.00 %	Mixed type	40
10	Vicia Sativa	1000ppm	0.5M HCl	91.24 %		Mixed type	41
11	A flavonoid	1 mM	1M HCl	95.00 %		Mixed type	42
12	Chitosan Schiff base	50 ppm	1M HCl	90.65 %		Mixed type	43
13	Carbon dots	200 mg/mL	1M HCl	92.36 %	-	Mixed type	44
14	Myristic-acid-based-imidazoline	400 ppm	5M HCl	95.60 %		Mixed type	45
15	BTC-SBCOE	5 mM	2M HCl	95.73 %	96.42 %	Mixed type	This Work